

Predictions for high-energy real and virtual photon-photon scattering from color dipole BFKL-Regge factorization

N. N. Nikolaev^{1,2}, J. Speth¹ and V. R. Zoller²

¹ Institut für Kernphysik, Forschungszentrum Jülich,
D-52425 Jülich, Germany

E-mail: kph154@ikp301.ikp.kfa-juelich.de

² Landau Institute for Theoretical Physics, Chernogolovka, Moscow Region 142 432,
Russia

³ Institute for Theoretical and Experimental Physics,
Moscow 117218, Russia
E-mail: zoller@heron.itep.ru

Abstract

High-energy virtual photon-virtual photon scattering can be viewed as interaction of small size color dipoles from the beam and target photons, which makes ; scattering at high energies (LEP, LEP 200 & NLC) an indispensable probe of short distance properties of the QCD pomeron exchange. Based on the color dipole representation, we investigate consequences for the ; scattering of the finding by Fadin, Kuraev and Lipatov that incorporation of asymptotic freedom into the BFKL equation makes the QCD pomeron a series of isolated poles in the angular momentum plane. The emerging color dipole BFKL-Regge factorization allows us to relate in a model-independent way the contributions of each BFKL pole to ; scattering and DIS on protons. Numerical predictions based on our early work on color dipole BFKL phenomenology of DIS on protons gives a good agreement with the recent experimental data from OPAL and L3 experiments at LEP 200. We discuss the salient features of the BFKL-Regge expansion for ; scattering including the issue of possible dominance of the rightmost BFKL pomeron contribution.

1 Introduction

In this note we study scattering of virtual and real photons

$$(q) + (p) \rightarrow X : \quad (1)$$

in the high-energy Regge regime. The standard definition of the cosine of the scattering angle in the t-channel suggests strongly that large Regge parameter $\frac{1}{x}$ depends on virtualities of photons as [1]

$$\frac{1}{x} = \frac{W^2 + Q^2 + P^2}{Q^2 + P^2 + m^2} \quad 1: \quad (2)$$

where $W^2 = (q + p)^2$ is the center-of-mass energy squared of colliding space-like photons (q) and (p) with virtualities $q^2 = Q^2$ and $p^2 = P^2$, respectively. The mass of the meson squared sets the natural scale for real photons.

The recent strong theoretical [2, 3, 4, 5, 6] and experimental [7, 8, 9, 10], see also a compilation in [11] interest in high-energy ; ; scattering stems from the fact that virtualities of photons give a handle on the size of color dipoles in the beam and target photons and, eventually, on short distance properties of the QCD pomeron exchange. For earlier development of the subject see the pioneering paper [12].

As noticed by Fadin, Kuraev and Lipatov in 1975 [13] and discussed in more detail by Lipatov in [14] the incorporation of asymptotic freedom into the BFKL equation makes the QCD pomeron a series of isolated poles in the angular momentum plane. The contribution of each isolated pole to the high-energy scattering amplitude satisfies the familiar Regge factorization [15]. In [16] we reformulated the consequences of the Regge factorization in our color dipole (CD) approach to the BFKL pomeron. In this communication we address several closely related issues in photon-photon scattering in the Regge regime (2) which can be tested at LEP 200 and Next Linear Collider (NLC). First, following our early work [16, 17, 18] we discuss how the color dipole (CD) BFKL-Regge factorization leads to the parameter-free predictions for total cross sections of ; ; scattering. We find good agreement with the recent experimental data from the L3 and OPAL experiments at LEP [7, 8, 9, 10]. Second, we discuss the onset of hard scattering regime with increasing virtualities of photons. The nodal properties of eigenfunctions of the CD BFKL equation suggest an interesting possibility of isolating the rightmost BFKL pole contribution when the virtuality of one or both of photons is in the broad vicinity of $Q^2 = 20 \text{ GeV}^2$. Third, we discuss the impact of running CD BFKL on contentious issue of testing the factorization properties of photon-photon scattering in the $Q^2; P^2$ plane which has earlier been discussed [5] only in the approximation of $s = \text{const}$ to the BFKL equation.

2 Overview of color dipole BFKL-Regge factorization

In the color dipole basis the beam-target scattering is viewed as interaction of color dipoles r and r^0 in both the beam (b) and target (t) particles, where r and r^0 are the two-dimensional vectors in the impact parameter plane. As a fundamental quantity we use the forward dipole scattering amplitude and/or the dipole-dipole cross section $\langle x; r; r^0 \rangle$. Once $\langle x; r; r^0 \rangle$ is known the total cross section of $b\bar{t}$ scattering $\sigma^{b\bar{t}}(x)$ is calculated as

$$\sigma^{b\bar{t}}(x) = \int dz d^2r dz^0 d^2r^0 j_b(z; r) j_t(z^0; r^0) \langle x; r; r^0 \rangle : \quad (3)$$

In the color dipole factorization formula (3) the dipole-dipole cross section $\langle x; r; r^0 \rangle$ is beam-target symmetric and universal for all beams and targets, the beam and target dependence is concentrated in probabilities $j_b(z; r)$ and $j_t(z^0; r^0)$ to find a color dipole, r and r^0 in the beam and target, respectively. Hereafter we focus on cross sections averaged over

polarizations of the beam and target photons, in this case only the term $n = 0$ of the Fourier series

$$(x; r; r^0) = \sum_{n=0}^{\infty} a_n(x; r; r^0) \exp(in\theta'); \quad (4)$$

where θ' is an azimuthal angle between r and r^0 , contributes in (3).

Fadin, Kuraev and Lipatov noticed in 1975 [13], see also Lipatov's extensive discussion [14] that the incorporation of asymptotic freedom into the BFKL equation makes the QCD pomeron a series of isolated poles in the angular momentum plane. The contribution of the each pole to scattering amplitudes satisfies the standard Regge factorization [15], which in the CD basis implies the CD BFKL-Regge expansion for the vacuum exchange dipole-dipole cross section

$$(x; r; r^0) = \sum_{m=0}^{\infty} C_m(x) \delta_m(r^0) \frac{x_0^m}{x^m}; \quad (5)$$

Here the dipole cross section $\delta_m(r)$ is an eigenfunction of the CD BFKL equation [16, 17, 19, 20, 21]

$$\frac{\partial \delta_m(x; r)}{\partial \log(1/x)} = K \delta_m(x; r) = \omega_m(x; r); \quad (6)$$

with eigen value (intercept) ω_m .

For the details on CD formulation of the BFKL equation, infrared regularization by finite propagation radius R_c for perturbative gluons and freezing of strong coupling at large distances, the choice of the physically motivated boundary condition for the hard BFKL evolution and description of eigenfunctions we refer to our early works [16, 17, 21], the successful application of CD BFKL-Regge expansion to the proton and pion structure functions and evaluation of hard-pomeron contribution to the rise of hadronic and real photoabsorption cross sections is found in [21, 16, 17, 18]. We only recapitulate the salient features of the formalism essential for the present discussion.

There is a useful analogy between the intercept $\omega_0 = (0) = 1$ and binding energy for the bound state problem for the Schrodinger equation. The eigenfunction $\delta_0(r)$ for the rightmost hard BFKL pole (ground state) corresponding to the largest intercept $\omega_0 = \omega_p$ is node free. The eigenfunctions $\delta_m(r)$ for excited states with m radial nodes have intercept $\omega_m < \omega_p$. Our choice of $R_c = 0.27 \text{ fm}$ yields for the rightmost hard BFKL pole the intercept $\omega_0 = 0.4$, for subleading hard poles $\omega_m = \omega_0 = (m + 1)$. The node of $\delta_1(r)$ is located at $r = r_1 \approx 0.05 - 0.06 \text{ fm}$, for larger m the rightmost nodes move to a somewhat larger r and accumulate at $r \approx 0.1 \text{ fm}$, for the more detailed description of the nodal structure of $\delta_m(r)$ see [16, 17]. Here we only emphasize that for solutions with $m \geq 3$ the third and higher nodes are located at a very small r way beyond the resolution scale $1 = \frac{p}{Q^2}$ of foreseeable DIS experiments. Because in the attainable region of r the subleading solutions $m \geq 3$ can not be resolved and they all have similar intercepts $\omega_m \approx 1$, in practical evaluation of $\hat{F}(x)$ we can truncate expansion (5) at $m = 3$ lumping in the term with $m = 3$ contributions of all singularities with $m \geq 3$. Such a truncation can be justified a posteriori if such a contribution from $m \geq 3$ turns out to be a small correction, which will indeed be the case at very small x . Notice that the Regge cut in the complex angular momentum plane found in the much discussed approximation $s = \text{const}$ resembles an infinite, and continuous, sequence of poles. In the counterpart of our CD BFKL-Regge expansion (5) for approximation $s = \text{const}$ the intercept ω_m would be a continuous parameter in contrast to a discrete spectrum for standard running s .

Because the BFKL equation sums cross sections of production of multigluon final states, the perturbative two-gluon exchange is an arguably natural boundary condition. This leaves the starting point x_0 as the only free parameter which fixes completely the result of the hard BFKL evolution for dipole-dipole cross section. We follow the choice $x_0 = 0.03$ made in [21]. The very ambitious program of description of $F_{2p}(x; Q^2)$ starting from this, perhaps excessively restrictive, perturbative two-gluon boundary condition has been launched by us in [16] and met with remarkable phenomenological success [17, 18].

Whereas scattering of small dipoles $r < R_c$ is dominated by the exchange of perturbative gluons, interaction of large dipoles has been modeled in Ref.[21, 17] by the factorizable non-perturbative soft pomeron with intercept $\alpha_{soft}(0) = 1 = \alpha_{soft} = 0$. Then the extra term $C_{soft,soft}(r) \alpha_{soft}(r^0)$ must be added in the r.h.s. of expansion (5). The exchange by two non-perturbative gluons [23] has been behind the parameterization of $\alpha_{soft}(r)$ suggested in [21, 22] and used later on in [16, 18] and here. For related recent models for soft pomeron cross section $\alpha_{soft}(r)$ see [24] and [25].

Finally, at moderately small values of x the above described t-channel gluon exchange pomeron must be complemented by the t-channel non-vacuum reggeon, i.e., $q\bar{q}$ exchange associated with DIS or quasi-valence quarks in the target and/or the Quark Parton Model component as it is often referred to in the literature on photon-photon scattering. The detailed phenomenology of this component is found in [2] and references therein, in our evaluations we use the parameterization developed in [2].

Then, combining (5) and (3) and adding in the soft and quasi-valence (reggeon) components, we obtain our principal result for virtual-virtual scattering ($m = \text{soft}; 0; 1; 2; \dots$)

$$\begin{aligned} (x; Q^2; P^2) &= \sum_m C_m f_m(Q^2) f_m(P^2) \frac{3x_0}{2x} + F_{2m}^{\text{qval}}(x; Q^2; P^2) \\ &= \frac{(4\pi)^2 \alpha_m}{Q^2 P^2} \sum_m C_m f_m(Q^2) f_m(P^2) \frac{3x_0}{2x} + F_{2m}^{\text{qval}}(x; Q^2; P^2); \end{aligned} \quad (7)$$

and DIS or (quasireal) real photons, $P^2 = 0$,

$$F_2(x; Q^2) = \sum_m A_m f_m(Q^2) \frac{3x_0}{2x} + F_2^{\text{qval}}(x; Q^2); \quad (8)$$

$$(x; Q^2; P^2) = \sum_m C_m f_m(Q^2) f_m(P^2) \frac{3x_0}{2x} + F_{2m}^{\text{qval}}(x; Q^2; P^2); \quad (9)$$

Here ($m = \text{soft}; 0; 1; 2; \dots$)

$$f_m(Q^2) = h_T j_m(r) j_T i + h_L j_m(r) j_L i; \quad (10)$$

are calculated with the well known color dipole distributions in the transverse (T) and longitudinal (L) photon of virtuality Q^2 derived in [23], and the eigen structure functions are defined as usual:

$$f_m(Q^2) = \frac{Q^2}{4\pi^2 \alpha_m} h_m(Q^2); \quad (11)$$

The factor $\frac{3}{2}$ in the Regge parameter derives from the point that in a scattering of color dipole on the photon the effective dipole-dipole collision energy is $\frac{3}{2}$ of that in the reference

scattering of color dipole on the three-quark nucleon at the same total cm.s. energy W . The analytical formulas for eigen structure functions $f_m(Q^2)$ are found in the Appendix. We do not need any new parameters compared to those used in the description of DIS and real photoabsorption on protons [16, 17, 18], the results for the expansion parameters A_m and $\alpha_m(0)$ are summarized in table 1.

We recall that because of the diffusion in color dipole space, exchange by perturbative gluons contributes also to interaction of large dipoles $r > R_c$ [20]. However at moderately large Regge parameter this hard interaction driven effect is still small. For this reason in what follows we refer to terms $m = 0; 1; 2; 3$ as hard contribution as opposed to the genuine soft interaction.

Table 1. CD BFKL-Regge expansion parameters.

n	m	$P_m; mb$	$C_m; mb^{-1}$	$A_m = \alpha_m$	$\alpha_m; b$	$\alpha_m; nb$
0	0.40	1.243	0.804	0.746	6.767	36.84
1	0.220	0.462	2.166	0.559	1.885	7.69
2	0.148	0.374	2.674	0.484	1.320	4.65
3	0.111	0.993	1.007	0.440	3.186	10.22
soft	0.	31.19	0.0321	0.351	79.81	204.2

3 Isolating the rightmost hard BFKL pole in highly virtual-virtual scattering

We start with the theoretically cleanest case of the highly virtual photons, $P^2; Q^2 \gg 1 \text{ GeV}^2$ and focus on the vacuum exchange component of the total cross section. Because of the well known BFKL diffusion in the color dipole space, hard scattering contributes to interaction of large color dipoles and soft scattering contributes to interaction of perturbatively small color dipoles. However, the soft interaction background diminishes at large $P^2; Q^2$. Furthermore, the CD BFKL approach with asymptotic freedom predicts uniquely that subleading eigen structure functions have a node at $Q^2 \approx 20 \text{ GeV}^2$ in which region of Q^2 the rightmost hard pole contribution will dominate. This suppression of the soft pomeron and subleading hard background is shown in Fig. 1, in which we plot the ratio ($m = 1; 2; 3; \text{soft}$)

$$r_m(Q^2) = \frac{f_m(Q^2)}{f_0(Q^2)} \frac{\overline{C_m}}{\overline{C_0}};$$

which defines the size of the soft and subleading hard background to the rightmost hard BFKL contribution at $x = x_0$. At this value of x the contribution of subleading hard BFKL poles remains marginal in a broad range of Q^2 , although the contribution from the single-node component $m = 1$ becomes substantial at $q^2 > 10^3 \text{ GeV}^2$. The soft-pomeron exchange contributes substantially at $Q^2 < 1 \text{ GeV}^2$ and dominates at $Q^2 \approx 0$. However, at very large $W \approx 100 \text{ GeV}$ of the practical interest at LEP and LHC, such small values of Q^2 correspond to extremely small x , where the soft and subleading hard contributions are Regge suppressed by the factor $\frac{x}{x_0}^{-p}$ and $\frac{x}{x_0}^{-0.5-p}$, respectively.

According to the results shown in Fig. 1 the dominance of the rightmost hard BFKL pomeron exchange in virtual-virtual scattering holds in a very broad range of $3 < Q^2; P^2 < 300 \text{ GeV}^2$ which nearly exhausts the interesting kinematical region at LEP 200

and N_{LC} . In this range of $P^2; Q^2$ we predict the vacuum exchange contribution of explicitly factorized form

$$(x; Q^2; P^2) = \frac{(4^2 \pi^2)^2 f_0(Q^2) f_0(P^2) C_0}{Q^2 P^2} \frac{3x_0}{2x}^0, \quad 1.57 \text{ nb} \quad \frac{G \text{ eV}^4}{Q^2 P^2}^! \quad \frac{W^2}{Q^2 + P^2}^! 0.4$$

$$(" \quad 1 + 0.326 \log \frac{1 + \frac{1.12 Q^2}{G \text{ eV}^2}}{1 + 0.326 \log \frac{1 + \frac{1.12 P^2}{G \text{ eV}^2}}{1 + \frac{1.12 P^2}{G \text{ eV}^2}}})^{\frac{10}{3}} \quad (12)$$

The quality of dominance of the rightmost hard BFKL pole exchange can be judged also from fig. 2 for the diagonal case of $Q^2 = P^2$, in which we show separately the soft component of the cross section (the dashed curve). The point that the contribution from subleading hard BFKL exchange is marginal is clear from the finding that approximation of soft-pomeron plus the rightmost hard BFKL exchange (LHSA) shown by long-dashed curve nearly exhausts the result from the complete CD BFKL-Regge expansion for vacuum exchange. Because of the very small values of x at $Q^2 < 1 \text{ GeV}^2$ the soft-pomeron exchange remains small down to $Q^2 = 0$, the quantitative discussion in this soft-soft regime requires better understanding of the unitarity corrections.

Recently the L3 collaboration [9] reported the first experimental evaluation of the vacuum exchange in equal virtuality scattering. Their procedure of subtraction of the non-vacuum reggeon and/or the quark Parton Model contribution is described in [9], arguably the subtraction uncertainties are marginal within the present errorbars. In fig. 3 we compare our predictions to the L3 data. The experimental data and theoretical curves are shown vs. the variable $Y = \log(\frac{W^2}{Q^2 P^2})$. The virtuality of two photons varies in the range of $1.2 \text{ GeV}^2 < Q^2; P^2 < 9 \text{ GeV}^2$ ($Q^2; P^2 \text{ in } 3.5 \text{ GeV}^2$) at $P \text{ in } 91 \text{ GeV}$ and $2.5 \text{ GeV}^2 < Q^2; P^2 < 35 \text{ GeV}^2$ at $P \text{ in } 183 \text{ GeV}$ ($Q^2; P^2 \text{ in } 14 \text{ GeV}^2$). We applied to the theoretical cross sections the same averaging procedure as described in [9]. The solid curve is a result of the complete BFKL-Regge expansion for the vacuum exchange, the dashed curve is a sum of the rightmost hard BFKL exchange and soft-pomeron exchange. The agreement of our estimates with the experiment is good, the contribution of subleading hard BFKL exchange is negligible within the experimental error bars.

The early calculations [5, 3, 4] of σ used the approximation $s = \text{const}$ which predicts the $P^2; Q^2$ -dependence different from our result (12) for CD BFKL approach with running s . Detailed comparison with numerical results by Brodsky, Hautmann and Soper (BHS) [5] is reported by the L3 Collaboration [9], which finds that BHS formulas overpredict substantially.

4 Virtual-real scattering: the rightmost hard BFKL pole in the photon structure function

The discussion of the photon structure function (SF) follows closely that of the proton and pion SF's in [16, 17, 18]. Our normalization of eigenfunctions is such that the vacuum (sea) contribution to the proton structure function ($m = \text{soft}; 0; 1; \dots; 3$)

$$F_{2P}(x; Q^2) = \sum_m^X f_m(Q^2) \frac{x_0}{x}^m \quad (13)$$

has the CD BFKL-Regge expansion coefficients $A_m^p = 1$. There is a fundamental point that the distribution of small-size color dipoles in the photon is enhanced compared to that in the proton [18] which enhances the importance of the rightmost hard BFKL exchange. Indeed, closer inspection of expansion coefficients A_m shown in table 1 reveals that subleading hard BFKL exchanges are suppressed by the factor 1.5 to 1.7, whereas the soft-pomeron exchange contribution is suppressed by the factor 3.

Our predictions for the photon structure function are parameter-free and are presented in fig. 4. At moderately small x there is a substantial non-vacuum reggeon exchange contribution from DIS or quasi-valence quarks which can be regarded as well constrained by the large x data, we use here the GRS parameterization [2]. The solid curve shows the result from the complete BFKL-Regge expansion the soft-pomeron (the dashed curve) and quasi-valence (the dot-dashed curve) components included, the dotted curve shows the rightmost hard BFKL (LH) plus soft-pomeron (S) plus quasi-valence (V) approximation (LHSVA). A comparison of the solid and dotted curves shows clearly that subleading hard BFKL exchanges are numerically small in the experimentally interesting region of Q^2 , the rightmost hard BFKL pole exhausts the hard vacuum contribution for $2 < Q^2 < 100 \text{ GeV}^2$. The nodal properties of subleading hard BFKL structure functions are clearly seen: LHSVA underestimates F_2 slightly at $Q^2 < 10 \text{ GeV}^2$ and overestimates F_2 at $Q^2 > 50 \text{ GeV}^2$. For still another illustration of the same nodal property of subleading hard components see fig. 5 in which we show the vacuum component of virtual-real total cross section σ_{tot} as a function of Q^2 at fixed W . As seen from fig. 1, the soft contribution rises towards small Q^2 , but this rise is compensated to a large extent by the small- x enhancement of the rightmost hard BFKL contribution by the large Regge factor $\frac{x}{x_0}^p$. For this region the soft background (the dashed curve) remains marginal over the whole range of Q^2 . Because of the node effect, the $m = 1$ subleading component changes the sign and becomes quite substantial at very large Q^2 and moderately small x . A comparison of the soft-hard decomposition of cross sections shown in fig. 2 and fig. 5 emphasizes the benefits of having the both photons virtual for the suppression of the soft-pomeron background to the hard BFKL exchange.

Recently the L3 and OPAL collaborations reported the first experimental data on the photon structure function at sufficiently small x [7, 10]. These data are shown in fig. 4 and are in good agreement with the predictions from the CD BFKL-Regge expansion. A comparison with the long-dashed curve which is the sum of the rightmost hard BFKL and soft exchanges shows that the experimental data are in the region of x and Q^2 still affected by non-vacuum reggeon (quasi-valence) exchange, going to smaller x and larger Q^2 would improve the sensitivity to pure vacuum exchange greatly.

5 The real-real scattering

We recall that because of the well-known BFKL diusion in color dipole space, exchange by perturbative gluons contributes also to interaction of large dipoles $r > R_c$ [20]. As discussed in [18] this gives rise to a substantial rising component of hadronic and real photoabsorption cross sections and a scenario in which the observed rise of hadronic and real photon cross sections is entirely due to this intrusion of hard scattering. This is a motivation behind our choice of intercept $\sigma_{\text{soft}} = 0$ for soft-pomeron exchange. Furthermore, in order to make this picture quantitative one needs to invoke strong absorption/unitarization to tame too a rapid growth of large dipole component of hard BFKL the dipole cross section. The

case of real-real scattering is not an exception and the above discussed enhancement of small dipole configurations in photons compared to hadrons predicts uniquely that the hard BFKL exchange component of real-real scattering will be enhanced compared to proton-proton and/or pion-proton scattering. This is clearly seen from table 1 in which we show the coefficients

$$m = m_m C_m \quad (14)$$

of the expansion for the vacuum exchange component of the total cross section

$$vac = \frac{x}{m} \frac{W^2 x_0}{m^2} \dots \quad (15)$$

One has to look at the soft-hard hierarchy of m and m_p in the counterparts of (15) for p and pp scattering. This enhancement of hard BFKL exchange is confirmed by simple vacuum pole plus non-vacuum reggeon exchange fits to real-real total cross section: the found intercept of the effective vacuum pole 0.21 is much larger than 0.095 from similar fits to the hadronic cross section data. In fig. 6 we compare our predictions from the CD BFKL-Regge factorization for the single-vacuum exchange contribution to real-real scattering with the recent experimental data from the OPAL collaboration [8] and [11]. The theoretical curves are in the right ballpark, but the truly quantitative discussion of total cross sections of soft processes requires better understanding of absorption/unitarization effects.

6 Regge factorization in and scattering

If the vacuum exchange were an isolated Regge pole, then the well-known Regge factorization would hold for asymptotic cross sections [15]

$$\frac{bb}{tot} \frac{aa}{tot} = \frac{ab}{tot} \frac{ab}{tot} \dots \quad (16)$$

In the CD BFKL approach such a Regge factorization holds for each term in the BFKL-Regge expansion for vacuum exchange, but evidently the sum of factorized terms does not satisfy the factorization (16). One can hope for an approximate factorization only provided one single term dominates in the BFKL-Regge expansion.

One such case is real-real scattering dominated by soft-pomeron exchange. For this reason the CD BFKL-Regge expansion which reproduces well the vacuum exchange components of the pp and p scattering can not fail for the vacuum component in real-real scattering. The rise of the contribution of hard-BFKL exchange breaks the Regge factorization relation

$$R = \frac{pp}{p} = 1; \quad (17)$$

which would restore at extremely high energies such that the rightmost hard BFKL exchange dominates. This property is illustrated in fig. 7 where we show our evaluation of R for single-vacuum component of total cross sections entering (16). At moderately high energies naive factorization breaks but the expected breaking is still weak, < 25%. This curve must not be taken at face value for $W > 0.1-1$ TeV because of likely strong absorption effects, but the trend of R being larger than unity and rising with energy should withstand unitarity effects.

The second case is highly virtual-virtual scattering. As we emphasized in section 3, here the CD BFKL approach predicts uniquely that because of the nodal property of subleading eigen structure functions the rightmost hard BFKL pole dominates the vacuum exchange in a broad range of $3 < Q^2; P^2 < 300 \text{ GeV}^2$, in which has a manifestly Regge factorized form (12). Equation (12) suggests clearly that different cross sections must be taken at the same value of the Regge parameter $\frac{1}{x}$, i.e., at the properly adjusted different values of W , in which case the vacuum components of scattering would satisfy

$$R(x) = \frac{[(x; Q^2; P^2)]^2}{(x; Q^2; Q^2)(x; P^2; P^2)} = 1 \quad (18)$$

In accordance to the results shown in g. 1, the subleading hard BFKL exchanges start contributing if either P^2 or Q^2 is either small, $< 3-5 \text{ GeV}^2$, or large, $> 50-100 \text{ GeV}^2$, and break the factorization relation (18). The breaking is weak, though, and breaking effects disappear rapidly, $\frac{1}{x} \rightarrow 0$, as $x \rightarrow 0$. If the vacuum singularity were the Regge cut as is the case in approximation $s = \text{const}$, then restoration of factorization is much slower, cf. our g. 8 and g. 9 of BHS [5]. The qualitative picture of factorization breaking is very similar, though, and we do not feel the factorization analysis can separate the two distinct models.

A comparison of scattering at fixed W would be somewhat misleading because different cross sections would enter at different values of the Regge parameter (2). Even if the rightmost hard BFKL dominates one would find

$$R(W) = \frac{[(W; Q^2; P^2)]^2}{(W; Q^2; Q^2)(W; P^2; P^2)} = R(x) \frac{2Q^2 P^2}{Q^2 + P^2} \Big|_{x=0} \quad (19)$$

Because $2 \approx 0.8$, the correction factor for rescaling of Regge parameters

$$= \frac{2Q^2 P^2}{Q^2 + P^2} \Big|_{x=0} \quad (20)$$

is quite substantial and its departure from unity can not be ignored. This rescaling of Regge parameters is different for the rightmost and subleading hard BFKL exchanges which further confuses the factorization tests done with cross sections taken at $W = \text{const}$.

For an obvious reason that the soft-pomeron exchange is so predominant in real-photon scattering, whereas the rightmost hard BFKL exchange is outstanding in virtual-virtual and real-virtual photon-photon scattering, it is ill advised to look at factorization ratios $R(x)/R(W)$ when one of the photons is quasireal, $P^2 \rightarrow 0$. In this limit one would find strong departures of $R(x)$ and $R(W)$ from unity. For precisely the same reason of predominance of soft-pomeron exchange in pp scattering vs. nearly dominant rightmost hard BFKL pole exchange in DIS at small x and $5-10 < Q^2 < 100 \text{ GeV}^2$, see [18], the naive factorization estimate

$$(W; Q^2; P^2) \frac{^P(W; Q^2) \quad ^P(W; P^2)}{^P(W)} \quad (21)$$

would not make much sense.

7 Conclusions

We explored the consequences for small- x photon structure functions $F_2(x; Q^2)$ and high-energy two-photon cross sections and from the color dipole BFKL-Regge factorization. Because of the nodal properties of eigen structure functions of subleading hard BFKL exchanges the CD BFKL approach predicts uniquely that the vacuum exchange is strongly dominated by the rightmost hard BFKL pole exchange in a very broad range of photon virtualities $Q^2; P^2$ which includes much of the kinematical domain attainable at LEP 200 and NLC. In this range of $Q^2; P^2$ the soft-pomeron exchange background is negligible small and the dominant vacuum exchange component is predicted to have the Regge factorized form. In general, the short-distance perturbative singularity in the photon wave function enhances the hard BFKL exchange and suppresses the soft-pomeron exchange background even for real photons. Starting with very restrictive perturbative two-gluon exchange as a boundary condition for BFKL evolution in the color dipole basis and having fixed the starting point of BFKL evolution in the early resulting CD BFKL-Regge phenomenology of the proton structure function, we presented parameter-free predictions for the vacuum exchange contribution to the photon structure function which agree well with OPAL and L3 determinations. A good agreement is found between our parameter-free predictions for the energy and photon virtuality dependence of the photon-photon cross section $(W; Q^2; P^2)$ and the recent data taken by the L3 Collaboration. We commented on the utility of Regge factorization tests of the CD BFKL-Regge expansion.

Acknowledgments: This work was partly supported by the grants INTAS-96-597 and INTAS-97-30494 and DFG 436RU S17/11/99.

Appendix

Although qualitative shape of eigenfunctions $f_m(r)$ as a function of r and/or eigenstructure functions $f_m(Q^2)$ as a function of Q^2 [16, 17] is well understood, they are only available as a numerical solution to the running color dipole BFKL equation. On the other hand, for the practical applications it is convenient to represent the results of numerical solutions for $f_m(Q^2)$ in an analytical form

$$f_0(Q^2) = a_0 \frac{R_0^2 Q^2}{1 + R_0^2 Q^2} \frac{h}{1 + c_0 \log(1 + r_0^2 Q^2)} \stackrel{i=0}{\dots} ; \quad (22)$$

$$f_m(Q^2) = a_m f_0(Q^2) \frac{1 + R_0^2 Q^2}{1 + R_m^2 Q^2} \stackrel{i=1}{\dots} \frac{1}{1 + \frac{z}{z_m}} \stackrel{!}{\dots} ; \quad m = 1; \quad (23)$$

where $m_{\max} = m_{\inf} ; 2g$, $g = \frac{4}{3}$ and

$$z = \frac{h}{1 + c_m \log(1 + r_m^2 Q^2)} \stackrel{i=m}{\dots} ; \quad m = 0; \quad (24)$$

The nodes of $f_m(Q^2)$ are spaced by 2-3 orders of magnitude in Q^2 -scale. The first nodes of sub-leading $f_m(Q^2)$ are located at $Q^2 \approx 20 - 60 \text{ GeV}^2$, the second nodes of $f_2(Q^2)$ and $f_3(Q^2)$ are at $Q^2 \approx 5 - 10 \text{ GeV}^2$ and $Q^2 \approx 2 - 10 \text{ GeV}^2$, respectively. The third node of $f_3(Q^2)$ is at $Q^2 \approx 2 - 10 \text{ GeV}^2$, way beyond the reach of accelerator experiments at small x . The parameters tuned to reproduce the numerical results for $f_m(Q^2)$ at $Q^2 < 10^5 \text{ GeV}^2$ are

listed in the Table 2. Form = 3 in this limited range of Q^2 we take a simplified form with only two first nodes.

Table 2. CD BFKL-Regge structure functions parameters.

n	a_m	c_m	$r_m^2 ; \text{GeV}^2$	$R_m^2 ; \text{GeV}^2$	$z_m^{(1)}$	$z_m^{(2)}$	m
0	0.0232	0.3261	1.1204	2.6018			1.
1	0.2788	0.1113	0.8755	3.4648	2.4773		1.0915
2	0.1953	0.0833	1.5682	3.4824	1.7706	12.991	1.2450
3	0.4713	0.0653	3.9567	2.7756	1.4963	6.9160	1.2284
soft	0.1077	0.0673	7.0332	6.6447			

The soft component of the proton structure function derived from $f_{\text{soft}}(r)$ of [22] is parameterized as follows

$$f_{\text{soft}}(Q^2) = \frac{a_{\text{soft}} R_{\text{soft}}^2 Q^2}{1 + R_{\text{soft}}^2 Q^2} \frac{h}{1 + c_{\text{soft}} \log(1 + r_{\text{soft}}^2 Q^2)} ; \quad (25)$$

with parameters cited in the Table 2.

References

- [1] P D B Collins, *Introduction to Regge Theory*. Cambridge University Press (1977)
- [2] M . G lück, E . R eya and I . Schienbein, *PhysRev.D* 60 (1999) 054019
- [3] J . Bartels , A . D e Ro eck and H . Lotter *PhysLett.B* 389 (1996) 742
- [4] J . Bartels , C . Ewerz , A . D e Ro eck and H . Lotter, e-Print Archive: [hep-ph/9710500](http://arxiv.org/abs/hep-ph/9710500)
- [5] S J . Brodsky, F . Hautmann and D E . Soper *PhysRevD* 56 (1997) 6957
- [6] B . Badelek , J . Kwieciński and A M . Stasto *Acta PhysPolon.B* 30 (1999) 1807
- [7] L3 Coll , M Acciarri et al , *Phys. Lett. B* 436 (1998) 403
- [8] OPAL Coll , G Abbiendi et al , CERN-EP/99-076 submitted to *EurPhys.J*
- [9] L3 Coll , M Acciarri et al , *Phys.Lett. B* 453 (1999) 333
- [10] OPAL Coll , K Ackersta et al , *Phys. Lett. B* 412 (1997) 225
- [11] Particle Data Group , *EurPhys.J.C* 3 (1998) 1
- [12] V M . Budnev , I F . G inzburg , G V M eledin and V G . Serbo , *PhysRep.* 15 (1975) 181
- [13] V S Fadin , E A Kuraev and L N Lipatov *Phys. Lett. B* 60 (1975) 50; E A Kuraev , L N Lipatov and V S Fadin , *Sov.Phys.JETP* 44 (1976) 443; 45 (1977) 199
- [14] L N . Lipatov , *Sov.Phys.JETP* 63 (1986) 904

[15] V N Gribov, B L Io e, I.Ya. Pom eranchuk and A P .Rudik, Sov Phys. JETP 16 (1963) 220

[16] N N .N ikolaev, B G .Zakharov, V R .Zoller, JETP Letters 66 (1997) 138.

[17] N N .N ikolaev and V R .Zoller, JETP Letters 69 (1999) 103; 176.

[18] N N .N ikolaev, J. Speth and V R .Zoller, e-Print Archive: hep-ph/9911433, Phys. Lett. B , in print.

[19] N N .N ikolaev, B G .Zakharov and V R .Zoller, JETP Letters 59 (1994) 8

[20] N N .N ikolaev, B G .Zakharov and V R .Zoller, JETP 105 (1994) 1498

[21] N N .N ikolaev and B G .Zakharov, Phys. Lett. B 327 (1994) 149; B 333 (1994) 250; B 327 (1994) 157.

[22] J. Nemchik, N N .N ikolaev, E .P redazzi, B G .Zakharov and V R .Zoller, JETP 86 (1998) 1054.

[23] N N .N ikolaev and B G .Zakharov, Z .Phys. C 49 (1991) 607.

[24] P V Landsho and O Nachtmann, Z .Phys. C 35 (1987) 405; H G Dosch, T Gousset, G Kulzinger and H J P imer Phys. Rev. D 55 (1997) 2602.

[25] A .D onnachie and P.V .Landsho , Phys.Lett. B 437 (1998) 408; K .G olic-B iemat and M .W ustho , Phys.Rev.D 59 (1999) 014017

[26] M .G luck, E .Reya and I. Schienbein, Eur. Phys. J. C 10 (1999) 313

Figure Captions

Fig.1 The normalized ratio of soft-to-rightmost hard and subleading hard-to-rightmost hard expansion coefficients ($m = 1, 2, 3$; soft) $r_m(Q^2) = \frac{f_m(Q^2)}{f_0(Q^2)} \frac{C_m}{C_0}$; of the BFKL-Regge expansion for scattering at $x = x_0$.

Fig.2 Predictions from CD BFKL-Regge expansion for the vacuum exchange component of the virtual-virtual cross section for the diagonal case of $Q^2 = P^2$ and for cms collision energy $W = 50, 100$ and 400 GeV (solid curves). The Leading Hard BFKL exchange plus Soft-pomeron exchange Approximation (LH SA) is shown by the long dashed curve. The soft-pomeron component of the cross section is shown separately by the dashed curve.

Fig.3 Predictions from CD BFKL-Regge expansion for the vacuum exchange component of the virtual-virtual cross section for the diagonal case of $hQ^2 i = hP^2 i$ are confronted to the experimental data by the L3 Collaboration [9]. The experimental data and theoretical curves are shown vs. the variable $Y = \log(W^2 = \frac{P^2}{Q^2 P^2})$.

Fig.4 Predictions from CD BFKL-Regge expansion for the photon structure function. The solid curve shows the result from the complete BFKL-Regge expansion the soft-pomeron (the dashed curve) and valence (the dot-dashed curve) components included, the dotted curve shows the rightmost hard BFKL (LH) plus soft-pomeron (S) plus quasi-valence (V) approximation (LH SVA). The long dashed line corresponds to the LH plus S approximation (LH SA). Data points are from [7, 10].

Fig.5 Predictions from CD BFKL-Regge expansion for the vacuum exchange component of the virtual-real total cross section and for cms collision energy $W = 50, 100$ and 400 GeV (solid curves). The result from the rightmost Hard BFKL (LH) plus Soft-pomeron (S) Approximation (LH SA) is shown by the long dashed curve. The soft-pomeron exchange component of the cross section is shown separately by the dashed curve.

Fig.6 Our predictions from the CD BFKL-Regge factorization for the single-vacuum exchange contribution to real-real scattering are compared with the recent experimental data from the OPAL collaboration [8] and [11].

Fig.7 Our evaluation of R for single-vacuum component of total cross sections.

Fig.8 The factorization cross section ratio $R(x)$ at fixed x and $Q = P$ as a function of $Q = P$ for $x = 10^2$ (dotted line), $x = 10^4$ (long-dashed) and $x = 10^6$ (dashed).

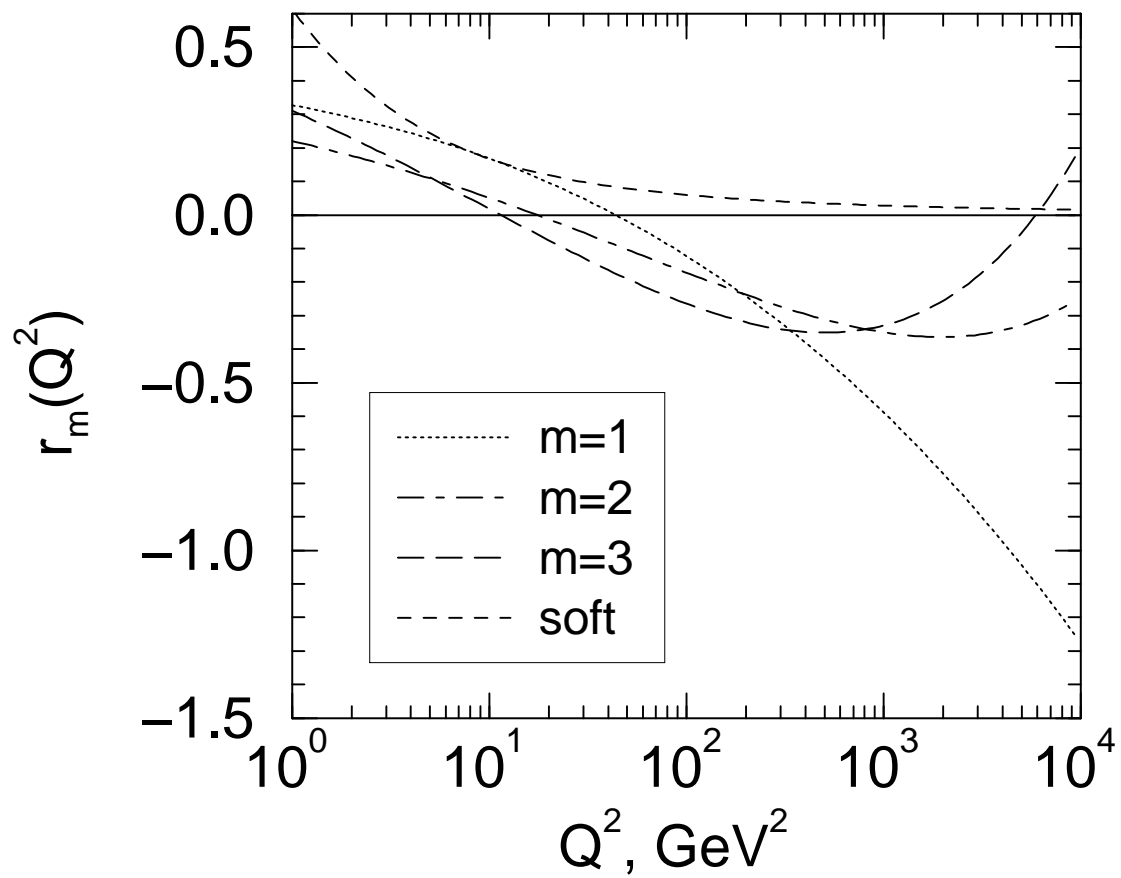


Fig. 1

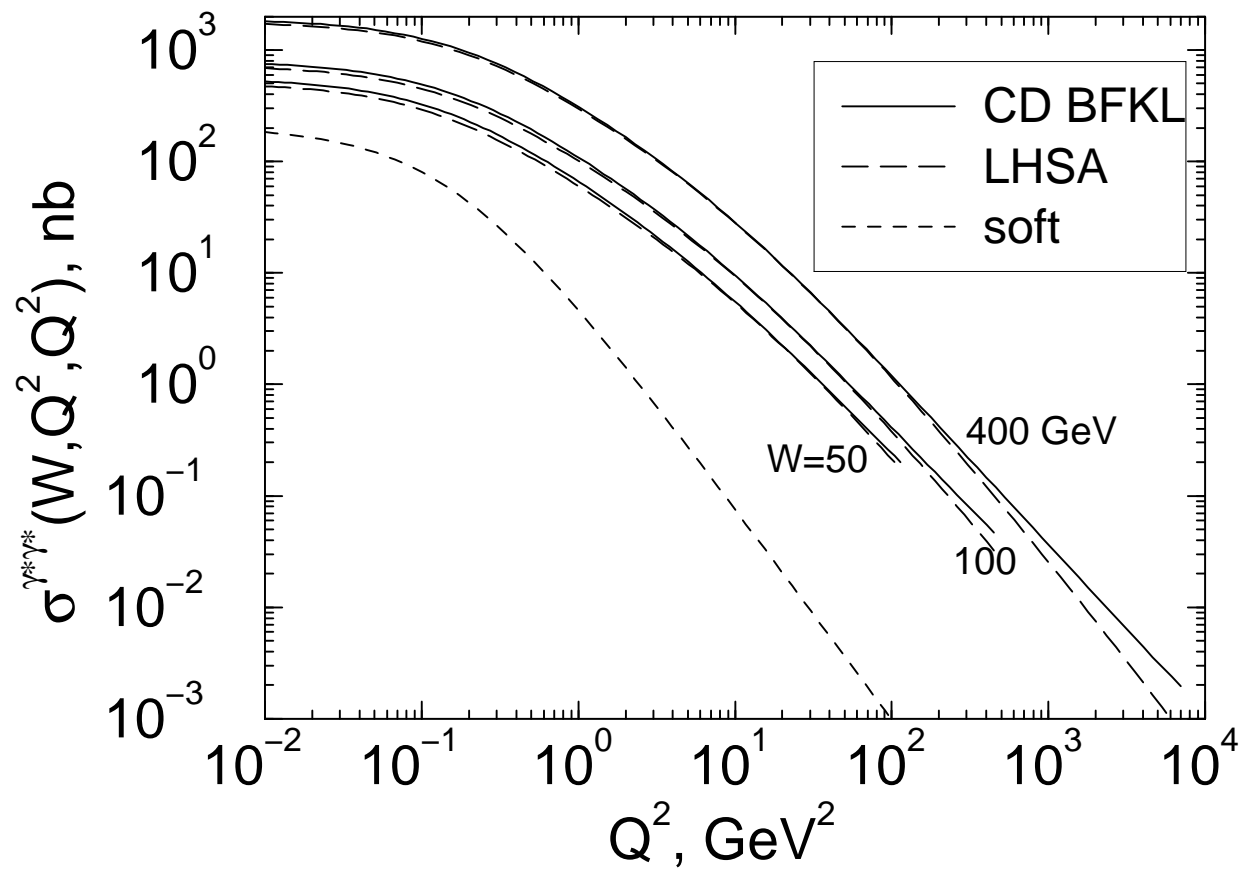


Fig. 2

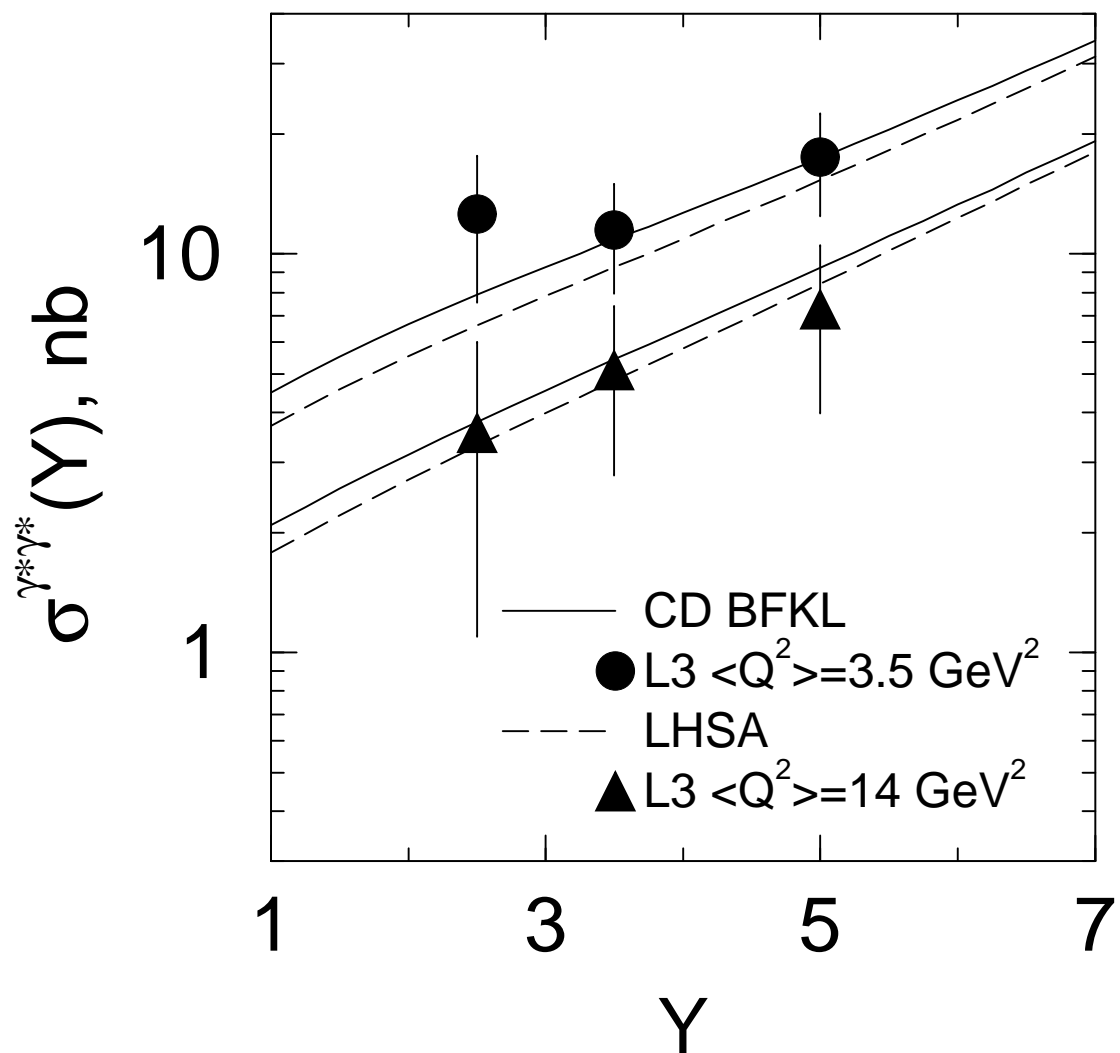


Fig. 3

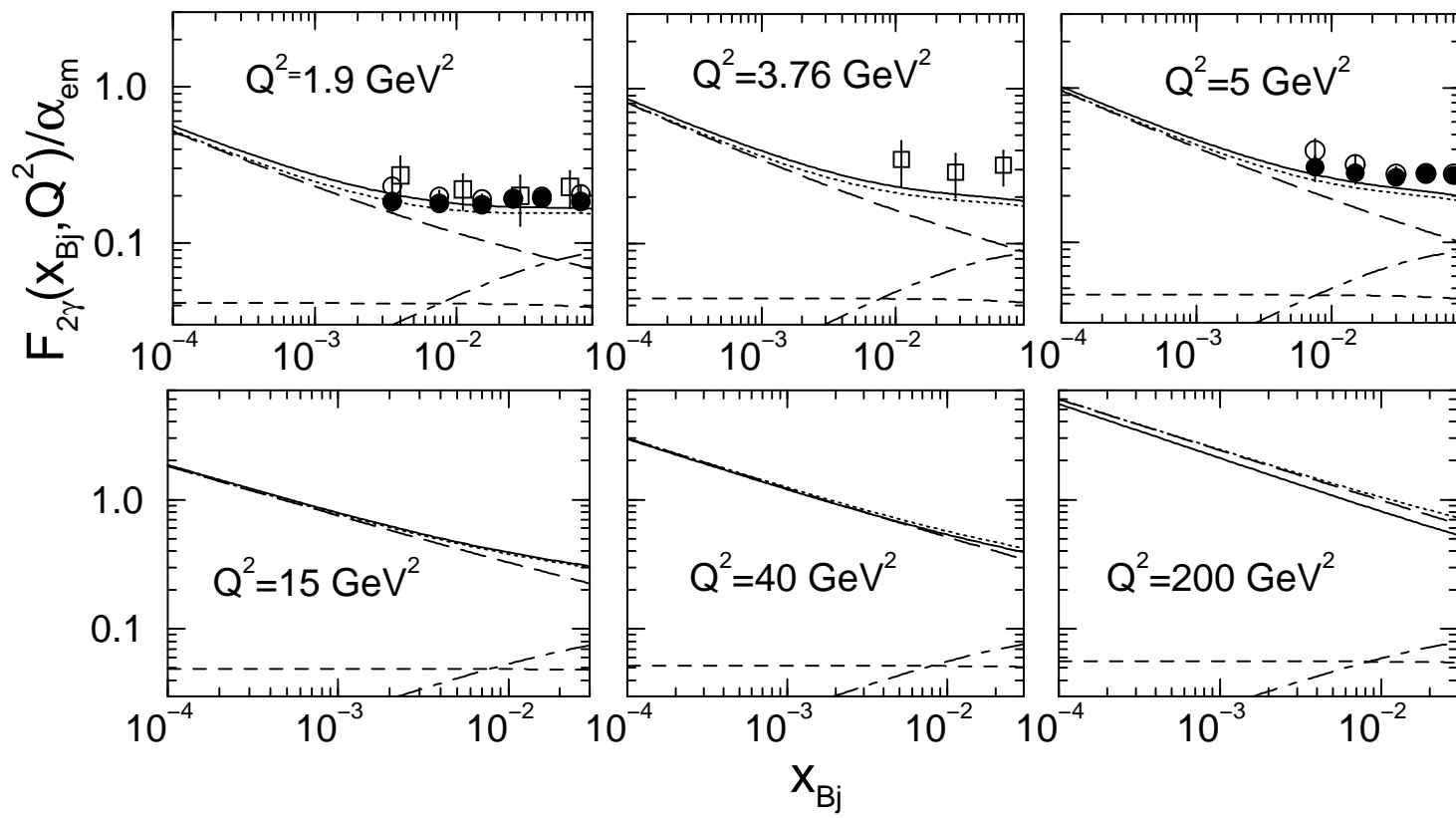


Fig. 4

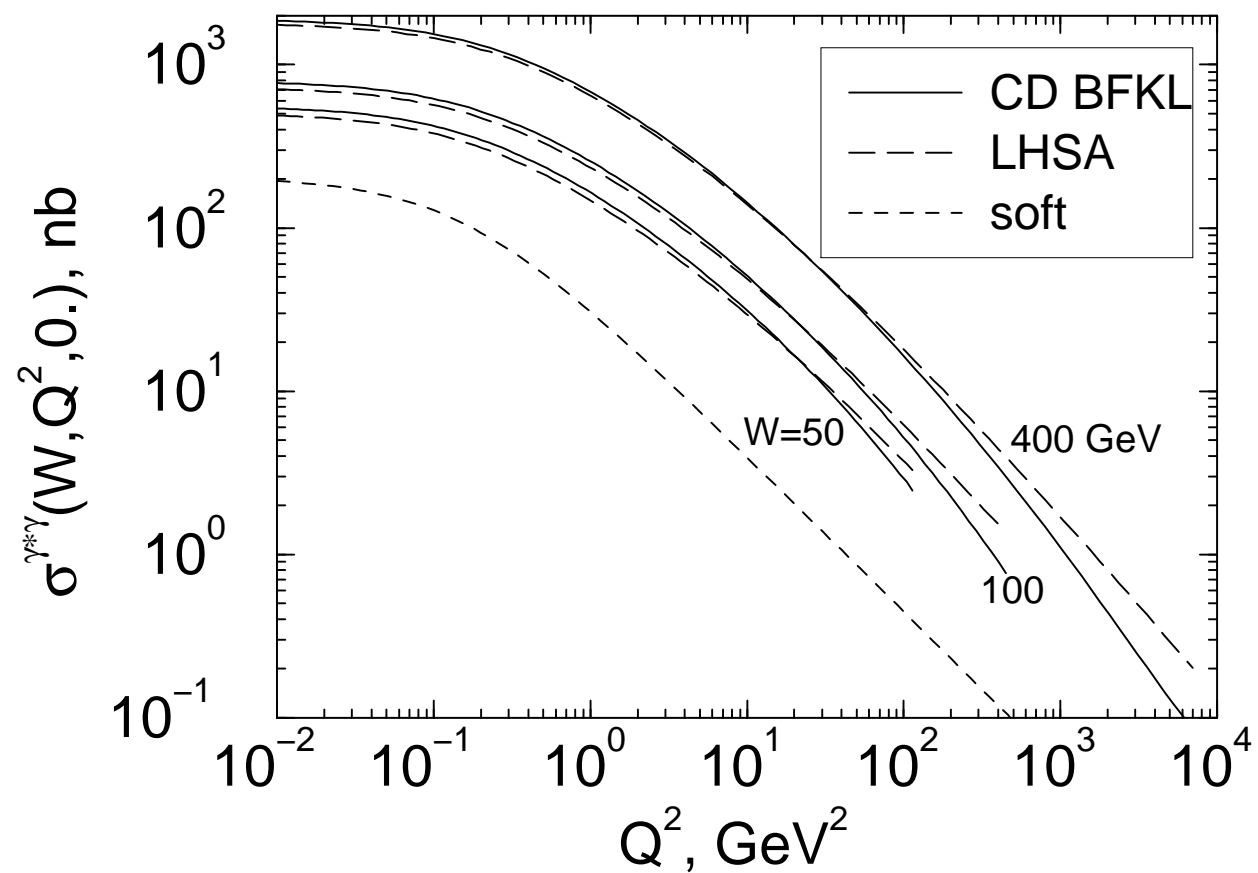


Fig. 5

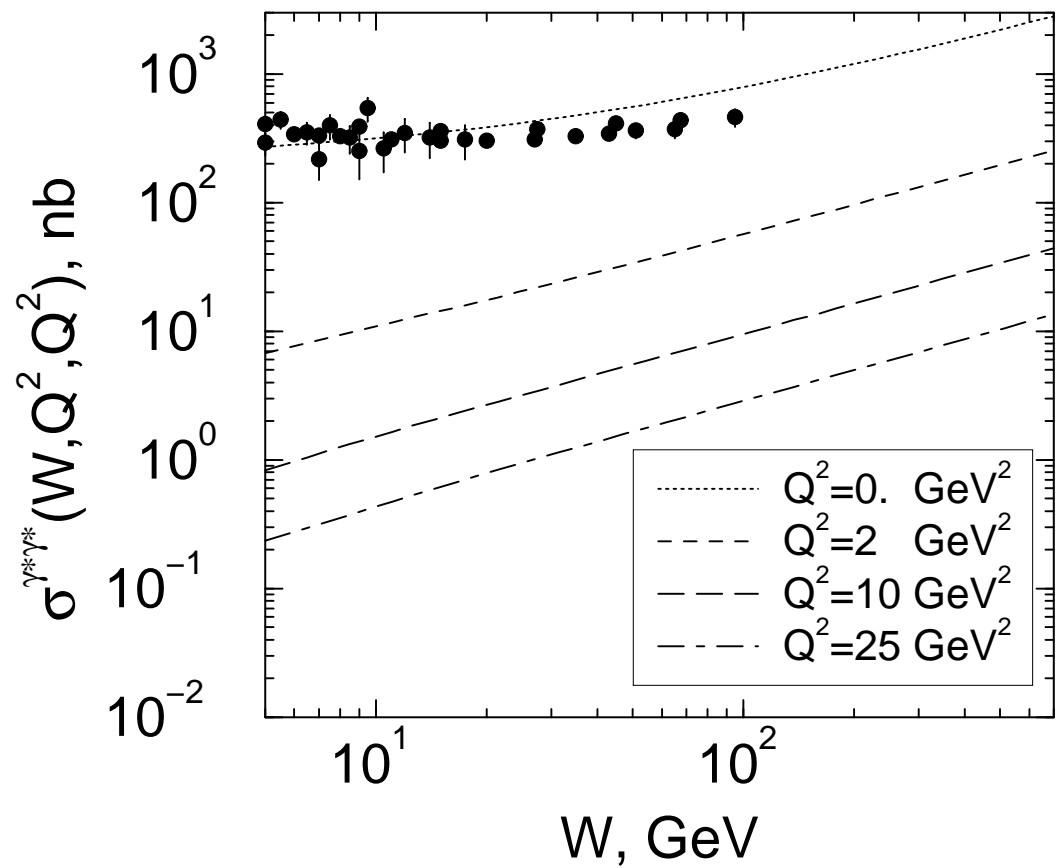


Fig. 6

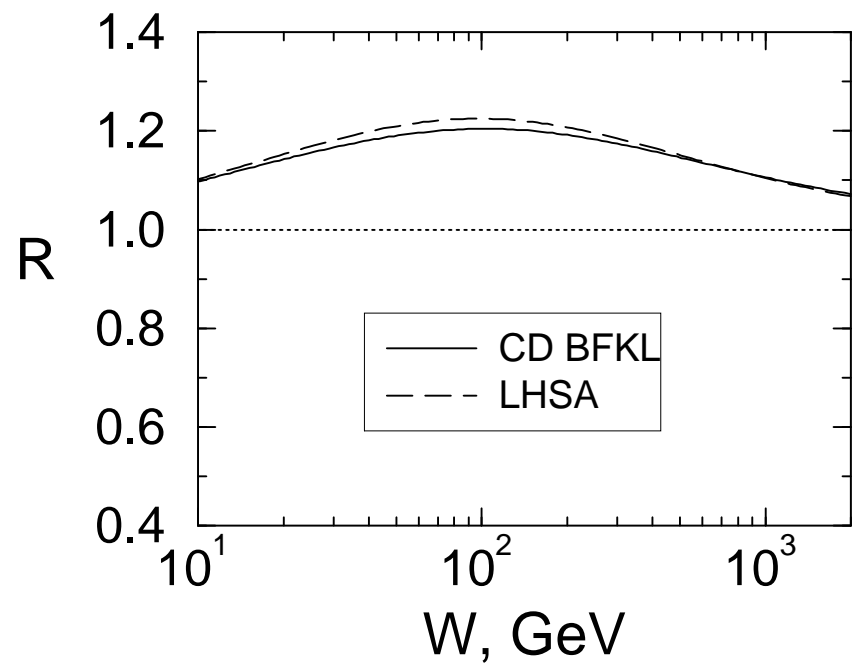


Fig. 7

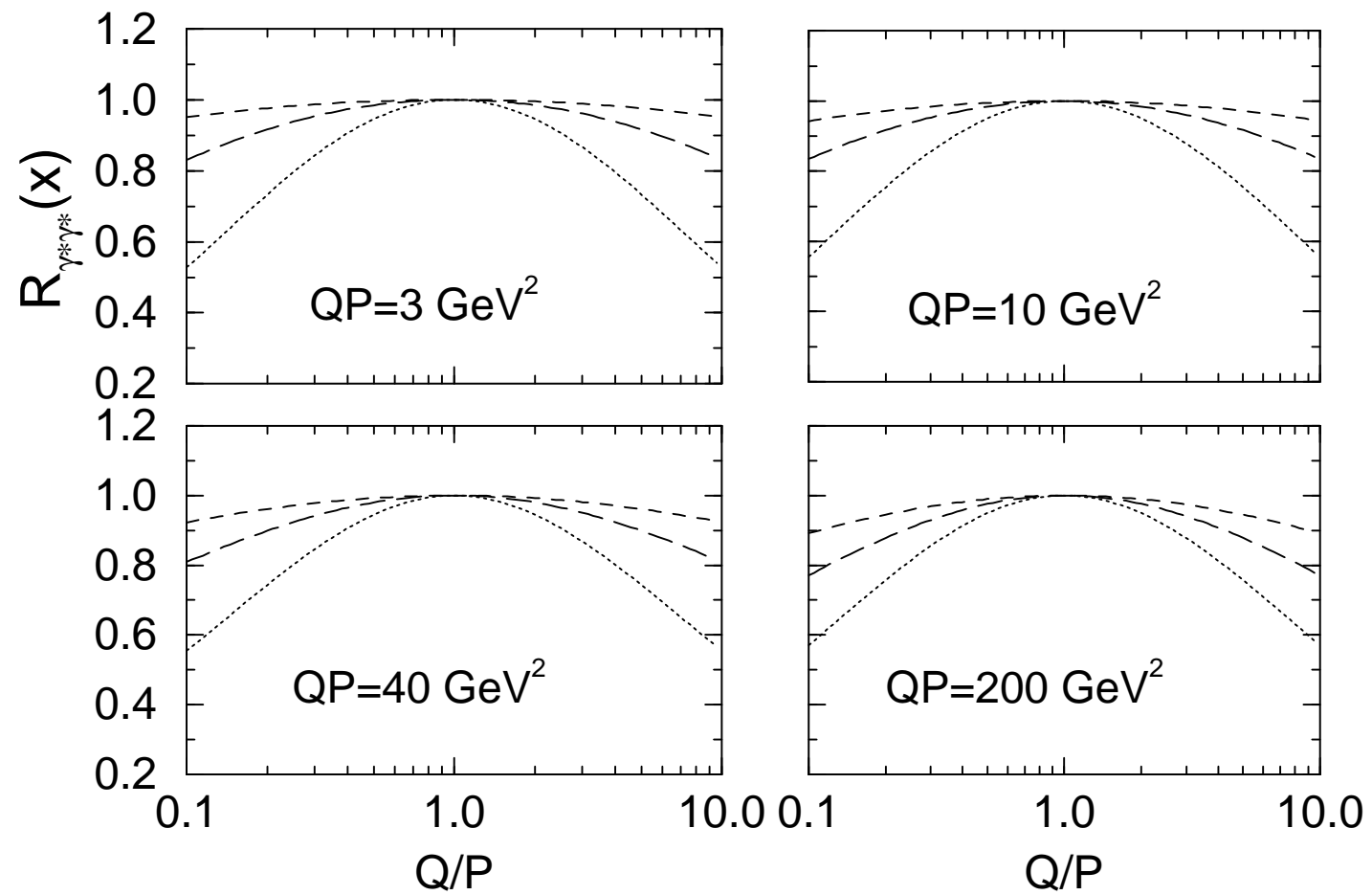


Fig. 8